Role of the tumour protein P53 gene in human cervical squamous carcinoma cells: Discussing haematopoietic cell-specific protein 1-associated protein X-1-induced survival, migration and proliferation

BING QIAN[1], LI-JUN ZHAO[1], FANG TENG[2], LING-JUAN GAO[2] and RONG SHEN[2]

[1]Department of Gynaecological Oncology, Jiangsu Cancer Hospital, Jiangsu Institute of Cancer Research, Nanjing Medical University Affiliated Cancer Hospital, Nanjing, Jiangsu 210009; [2]Department of Gynaecology, Nanjing Maternity and Child Health Care Hospital, Nanjing, Jiangsu 210004, P.R. China

Abstract. The haematopoietic cell-specific protein 1-associated protein X-1 (HAX-1), as a mitochondrial membrane protein, induces cancer progression and metastasis. The present study aimed to investigate the role of HAX-1-induced survival, migration and proliferation of human cervical squamous carcinoma cells and to elucidate its potential molecular mechanisms. The level of HAX-1 was examined by quantitative polymerase chain reaction and western blot analyses. The survival, migration and proliferation of the human cervical squamous carcinoma SiHa cell line were measured by the water-soluble tetrazolium salt (WST-1) assay, Transwell assay and ^{3}H-thymidine incorporation into DNA (^{3}H-TdR) assay, respectively. The intracellular reactive oxygen species (ROS) was estimated by the fluorescence of H_2DCFDA, and the mitochondrial membrane potential was tested using a JC-1 probe. The expression of the HAX-1 gene was significantly increased in human cervical carcinoma tissues relative to non-cancerous cervix tissues. Overexpression of HAX-1 increased the survival, migration and proliferation ability of SiHa cells, decreased the production of ROS, and maintained the integrity of the mitochondrial membrane and morphology. The effect brought on these cells could be abrogated by the addition of wild-type tumour protein P53 (p53) or carbonyl cyanide-p-trifluoro methoxyphenylhydrazone-induced mitochondrial dysfunction. In summary, these data support the notion that HAX-1 induced the survival, migration and proliferation of human cervical squamous carcinoma cells by inhibiting its downstream regulatory factor p53 in SiHa cells.

Introduction

Cervical cancer is one of the most serious diseases that threaten the physical and mental health of women. The morbidities and mortalities of cervical cancer rank first in China with >150,000 newly diagnosed cases annually, accounting for ~38% of the total number of cases worldwide (1,2). Aetiology studies have demonstrated that the incidence of cervical cancer is multi-factorial, involving multiple steps, and that the risk factors for cervical cancer may be associated with behavioural factors, biological factors and genetic susceptibility factors (3,4). Therefore, it is very important for the clinical diagnosis and treatment of cervical cancer to evaluate the associated mechanisms of the occurrence and development of cervical cancer.

The occurrence and development of tumours are associated with the pathological proliferation of cells and abnormal apoptosis (5,6). Once the balance between promoting apoptotic genes and inhibiting apoptotic genes is broken, tumours inevitably develop (6,7). Mitochondrial dysfunction is one of the key factors for apoptosis (8). Therefore, the present study investigated the role of mitochondrial dysfunction in the development of cervical cancer cells. Understanding the complex process of the regulation of a variety of signalling networks in the development and progression of cervical cancer is of great importance. As one of the key genes promoting apoptosis, tumour protein P53 (p53) serves an important role in controlling the cell cycle, inhibiting tumour formation, maintaining cell genome integrity and responding to various cellular stresses (9-12). In recent years, accumulating evidence has demonstrated that the p53 protein may translocate from the cytoplasm to the mitochondria and activate mitochondria-related apoptotic pathways. However, the p53-regulated genes that serve a major role in cervical cancer have not yet been identified.

Correspondence to: Dr Ling-Juan Gao or Dr Rong Shen, Department of Gynaecology, Nanjing Maternity and Child Health Care Hospital, 123 Tianfei Alley, Nanjing Mochou Road, Nanjing, Jiangsu 210004, P.R. China
E-mail: gaolingjuan@njmu.edu.cn

Haematopoietic cell-specific protein 1-associated protein X-1 (HAX-1) is a mitochondrial membrane protein with complex physiological functions and is also a potential oncogene (13). HAX-1 genes are overexpressed in numerous types of cancer and are involved in the tumorigenesis, growth, progression, invasion and metastasis of a number of human malignancies (14). The present study aimed to comprehensively determine the role of the p53 gene in HAX-1-induced biological behaviour of cervical cancer cells and the associated mechanism of mitochondrial function.

Materials and methods

Chemicals and reagents. The human cervical cancer SiHa cell line and the HeLa cell line were provided by the Hangzhou Hibio Bio-tech Co., Ltd (Hangzhou, China; http://www. hi-bio.cn/). The human cervical epithelial CRL2614cell line was purchased from American Type Culture Collection (ATCC, Manassas, VA, USA; http://www.atcc. org/Products/All/CRL-2614.aspx). The Lipofectamine® 2000 transfection reagent was purchased from Invitrogen; Thermo Fisher Scientific, Inc. (Waltham, MA, USA). A water-soluble tetrazolium salt (WST-1) kit, H_2DCFDA kit and JC-1kit were purchased from Invitrogen; Thermo Fisher Scientific, Inc. Antibodies againstHAX-1 (cat no. sc-166845), p53 and β-actin were purchased from Santa Cruz Biotechnology, Inc. (Dallas, TX, USA). Carbonyl cyanide-p-trifluoro methoxyphenylhydrazone (FCCP) was obtained from Tianjin Kaitong Chemical Reagent Co., Ltd. (Tianjing, China). The plasmids pCB6 + p53 encoding wild-type (wt) p53 and pCB6 + p53 173L encoding mutantp53 (mt) were supplied by Hangzhou Hibio Bio-tech Co., Ltd. The wild-type amino acid sequence prior to mutation for pCB6 + p53 173L was KQSQHMTEV (164-172). Transwell chambers were obtained from Invitrogen; Thermo Fisher Scientific, Inc. HAX-1 and β-actin gene primers were synthesized by Shanghai Boya Biotechnology Co., Ltd. (Shanghai, China; http://hkjum1210485.51sole.com/).

Tissue procurement and preparation. The present study was approved by the Ethics Committee of the Chinese Academy of Sciences and the Nanjing Maternity and Child Health Care Hospital (Nanjing, China) and written informed consent was obtained from all participants. Subsequently, the specimens were organized and case data were collected. Between December 2013 and October 2015, specimens of 24 cases (median age of 43 years, age range of 25-56 years) of cervical cancer and adjacent non-cancerous cervical tissues were collected at the Nanjing Maternity and Child Care Center Affiliated to Nanjing Medical University (Nanjing, China). All specimens were confirmed by pathological examination. The research specimens were divided into two groups: i) There were 24 cases of human cervical cancer tissues (T), the pathological diagnoses of which were definite, and ii) 24 cases of surrounding non-cancerous cervical tissues (N), with no tumour cell infiltration, confirmed by pathology. For cervical tissue analysis, the exclusion criteria was as follows: Positivity for *Chlamydia trachomatis*, *Neisseria gonorrhoeae*, *Gardnerella vaginalis*, *Mycoplasma genitalium*, *Trichomonas vaginalis*, *Mycoplasma pneumoniae* and Herpes simplex virus type 2 (HSV-2) sexually transmitted pathogens.

Immunohistochemical analysis. Immunohistochemistry for HAX-1in cervical cancer and adjacent non-cancerous cervical tissues was performed as follows: Dewaxing in fresh xylene (30 min at 55°C) and rehydration using an ethanol gradient (100, 95, 80 and 70%) for 2 min each at room temperature for antigen retrieval, the slides (2-3-μm-thick sections) were heated in a microwave oven in 0.02 M citrate buffer at pH 6.0. Subsequent to cooling, the sections were incubated in 3% perhydrol solution for 15 min at room temperature to block the endogenous peroxidase reaction. Non-specific binding was blocked for 1 h by incubation in 5% bovine serum albumin (Sigma Aldrich; Merck KGaA, Darmstadt, Germany) at room temperature. Then, the sections were incubated with mouse anti-human HAX-1 monoclonal antibody (dilution, 1:200; Santa Cruz Biotechnology, Inc. Dallas, TX, USA; cat. no. sc-166845) overnight at 4°C. The slides were then incubated with horseradish peroxidase-conjugated goat anti-mouse secondary antibody (dilution, 1:2,000; Santa Cruz Biotechnology, Inc.; cat. no. sc-2005) for 30 min at 37°C and 3,3'-diaminobenzidine Sigma-D8001 staining kit (Sigma Aldrich; Merck KGaA) staining was used for evaluation. The positive (brown) staining indicates the presence of the HAX-1 protein, as detected by light microscopy (magnification, x200).

Reverse transcription-quantitative polymerase chain reaction (RT-qPCR). Total RNA was extracted from cervical tissue using TRIzol® reagent (Invitrogen; Thermo Fisher Scientific, Inc.). The RNA was quantified by absorption at 260 nm. The isolated RNA was then DNase-treated and reverse-transcribed according to manufacturer's recommended protocol. To detect HAX-1, the following primer sets were used: Forward, 5'-CGCGGATCCAGTACGGGAATGAGCCCT-3' and reverse, 5'-ACGCGTCGACTTAACAAGGCTACCGGGA-3'. According to the HAX-1 mutated vector, a single point mutation for D148A (GAT->GCT) and D159A (GAC->GCC) was introduced to full-length HAX-1 that overlaps with the specific Asp residue that was changed to Ala. The mutant forward and reverse primers were as follows: D148A forward, 5'-TTGGAGAGTGCTGCAAGAAGTGAATCCCCCCAA-3' and reverse 5'-ACTTCTTGCAGCACTCTCCAAGACCCCCCCAAA-3'; and D159A forward, 5'-CCAGCACCAGCCTGGGGCTCCCAGAGGCCATTT-3' and reverse, 5'-GGAGCCCCAGGCTGGTGCTGGTTGGGGGGGATTC-3'. The sequence analysis was performed to confirm Asp to Ala conversions. Briefly, mRNA were reverse transcribed using a PrimeScript reverse transcription kit, miScript SYBR Green PCR kit and miScript primer assays according to the manufacturer's protocol (Qiagen, Inc., Valencia, CA, USA). RT-qPCR was performed using an ABI PRISM 7300 sequence detection system. Thermocycling parameters were 2 min at 50°C and 10 min at 95°C, followed by a total of 40 cycles of 15 s at 95°C and 1 min at 60°C. All of the reactions were performed in triplicate. The gene expression Cq values of mRNA were calculated by normalizing with the internal control of β-actin. The relative amounts of mRNA were calculated using the $2^{-\Delta\Delta Cq}$ method (15).

Electron microscopy. The cultured SiHa cells were trypsinized and pelleted at 800 x g for 15 min at 4°C. Following supernatant removal, the cell mass was post-fixed in 1% OsO_4 for 1 h

at room temperature and stained with 1% uranyl acetate for 2 h at room temperature. Next, the cell mass was dehydrated an acetone series (50, 70, 80, 90 and 100%) for 15 min each at room temperature, and flat-embedded in Durcupan (Fluka Chemie AG, Buchs, Switzerland) and sectioned to 60-70 nm thickness on 300 mesh copper slot grids. Finally, ultrathin sections were examined at magnifications of x3,700 and x12,500 and photographs were taken using a Zeiss 10^9 electron microscope (Carl Zeiss AG, Oberkochen, Germany).

Western blot analysis. The cultured SiHa cells were treated with pcDNA3.1-HAX-1 vector, pcDNA3.1-HAX-1 mutated vector and pcDNA3.1 vector for 72 h at 37˚C. Total protein of SiHa cells was extracted using radioimmunoprecipitation assay protein lysis buffer containing 150 mM NaCl, 1 mM Na_3VO_4, 50 mM NaF, 1% Triton X-100, 1mM EDTA, 1 mM PMSF, 10% glycerol, 20 mM Tris-HCl (pH 7.5) and protease inhibitors for 30 min on ice. An equal quantity of total protein (~20-30 µg, with the concentration of protein having been determined by a BCA protein assay, was subjected to 10% SDS-PAGE and transferred onto polyvinylidene difluoride membranes (EMD Millipore, Billerica, MA, USA). The membranes were blocked for 1 h in 5% skimmed milk dissolved in PBST (PBS containing 0.05% Tween 20) at room temperature. Following blocking, primary antibodies against HAX-1 (dilution, 1:400; cat. no. sc-166845), p53 (dilution, 1:500; cat. no. sc-47698) and β-actin (dilution, 1:500; cat. no. sc-69879) were applied to the membranes overnight at 4˚C. The proteins were visualized with horseradish peroxidase-conjugated goat anti-mouse secondary antibodies (dilution, 1:2,000; cat. no. sc-2005) for 1 h at room temperature using the enhanced chemiluminescence western detection system (Cell Signalling Technology, Inc., Danvers, MA, USA), including a biotinylated protein ladder, 20x LumiGLO reagent and 20x peroxide.

Cell survival analysis. The cultured SiHa cells were treated with pcDNA3.1-HAX-1 vector, pcDNA3.1-HAX-1 mutated vector and pcDNA3.1 vector for 72 h and examined for cell survival using a WST-1 assay. The WST-1 (10 µl/well) was added to each well and incubated at 37˚C for 4 h. The cell cultures were terminated and the culture supernatant was discarded. Dimethyl sulfoxide (150 µl) was added to the cell culture and incubated for 10 min to fully dissolve the reaction product. The absorbance was measured at an optical density (OD) of 490 nm using an automated microplate reader (Elx808; BioTek Instruments, Inc., Winooski, VT, USA).

SiHa cell migration analysis. The effect of different treatments on SiHa cell migration was measured by Transwell experiments. Prior to the test, the cultured SiHa cells ($7.5x10^6$ cells/ml) were starved for 24 h and placed in the upper well of a 6.5-mm Transwell chamber with 8-µm pores (Corning Incorporated, Corning, NY, USA). The upper chamber was filled with 100 µl serum-free DMEM and the lower chamber was filled with 500 µl culture medium containing 20% foetal bovine serum (FBS; Gibco; Thermo Fisher Scientific, Inc.), 1% nonessential amino acids and 2 mM glutamine. After 4 h of incubation, the migratory ability of SiHa cells was calculated by staining the adherent cells directly with 4% paraformaldehyde for 30 min at room temperature. The migrated cells were counted under the light microscope (magnification, x400) in five different fields per filter. The experiments were repeated 3-5 times.

Cell proliferation assay. The SiHa cells were treated with pcDNA3.1-HAX-1 vector (2 µg/ml), pcDNA3.1-HAX-1 mutated vector (2 µg/ml) and pcDNA3.1 vector (2 µg/ml) for 72 h and were serum starved for 24 h. DNA synthesis was measured by ^{3}H-thymidine incorporation (^{3}H-TdR; Hibio Bio-tech Co.) during the final 18-24 h. The cells were digested and collected onto glass fibre filter paper. The radioactivity retained on the dried filters was placed in liquid scintillation vial (a control vial was also used) containing 5 ml scintillation solution (Hibio Bio-tech Co.) and counted in a TopCount NxT scintillation counter (LKB Instruments, Mount Waverly, Victoria, Australia).

Assay of intracellular reactive oxygen species (ROS). A H_2DCFDA fluorescent probe kit was used to estimate ROS generation. The SiHa cells were treated with pcDNA3.1-HAX-1 vector (2 µg/ml), pcDNA3.1-HAX-1 mutated vector (2 µg/ml) and pcDNA3.1 vector (2 µg/ml) for 72 h and incubated with 10 µM H_2DCFDA at 37˚C for 20 min in the dark. The production of intracellular ROS was detected by inverted fluorescence microscopy (magnification, x200) with excitation at 488 nm and emission at 530 nm. The increase in fluorescence intensity with respect to normoxic untreated controls was calculated by subtracting the basal fluorescence levels.

Measurement of the mitochondrial membrane potential (Δψm). The loss of mitochondrial membrane potential (Δψm) was measured in SiHa cells using the fluorescent cationic dye JC-1 (Molecular Probes; Thermo Fisher Scientific, Inc.), which is a mitochondria-specific fluorescent dye. According to the manufacturer's protocols, treated SiHa cells were collected and stained with 10 µM JC-1 for 15 min at room temperature. Changes in JC-1 monomers were detected at the excitation wavelength 485 nm and the emission wavelength 530 nm under fluorescence microscopy (magnification, x200). The data are representative of 10 individual experiments.

Statistical analysis. SPSS 18 (SPSS, Inc., Chicago, IL, USA) and GraphPad Prism (GraphPad Software, Inc., La Jolla, CA, USA) were used for data analysis. The data are presented as the mean ± standard error of the mean. Quantitative data were analysed by one-way analysis of variance, followed by Tukey's post hoc test. P<0.05 was considered to indicate a statistically significant difference.

Results

HAX-1 gene expression in human cervical tissues. The results demonstrated that the level of HAX-1 mRNA and protein in cervical cancer tissues was significantly higher than that in adjacent cervical tissues (P<0.001; Fig. 1A and B). The location of HAX-1 protein was detected by IHC. Fig. 1C demonstrates that HAX-1 protein (brown staining) is predominantly expressed in the cytoplasm of cervical squamous cell carcinoma tissues, the positive ratio for these samples was ~75% of the immunohistochemical
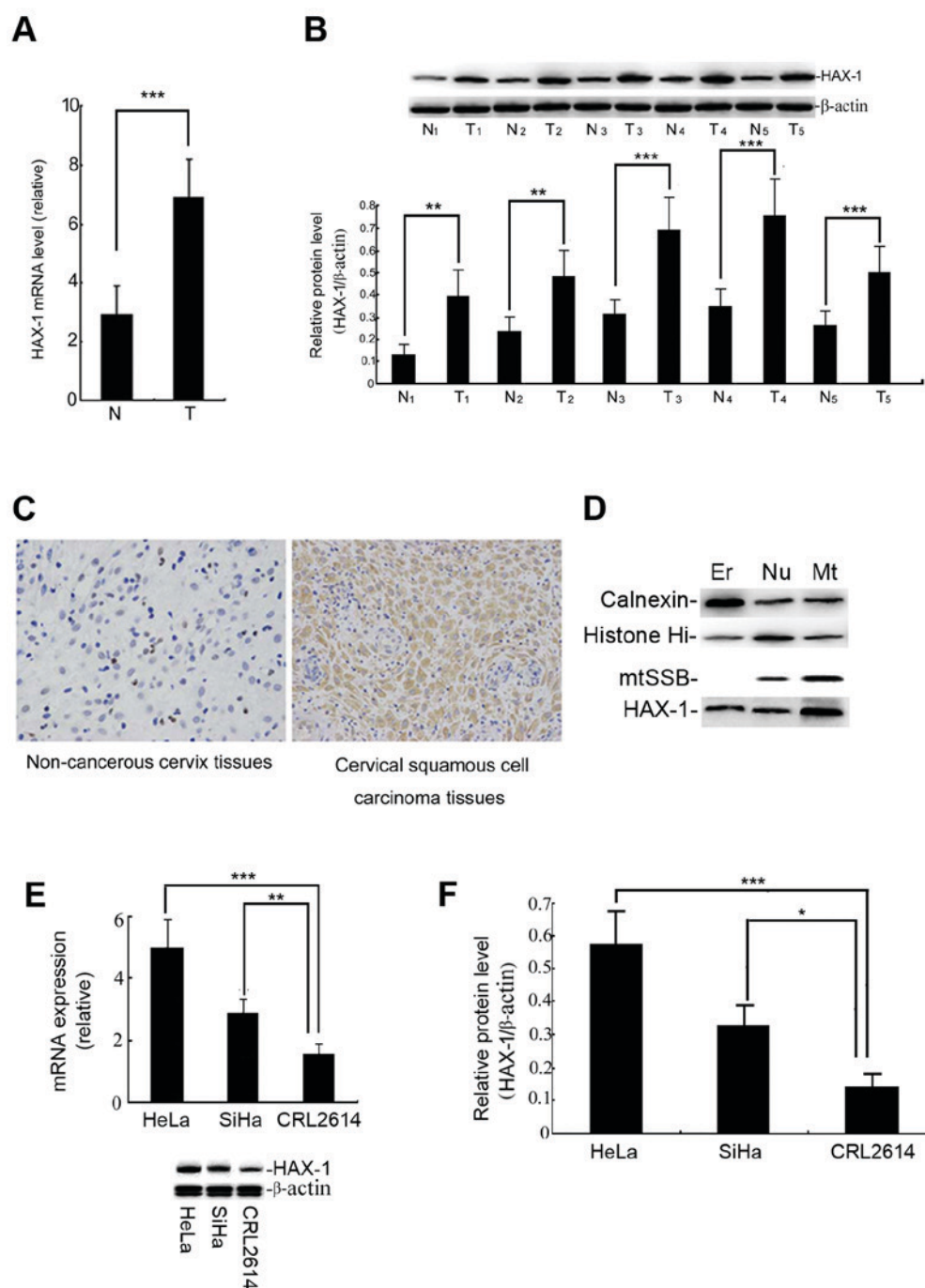
Figure 1. Expression level of the HAX-1 gene in human cervical tissues. (A) The relative HAX-1 gene levels in the T and N tissues. The level of HAX-1 mRNA was measured by qPCR. The results are presented as the mean ± SEM of three independent experiments, each conducted in triplicate. ***P<0.001. (B) The HAX-1 protein level was measured by western blot analysis. The graph was grey-scale scanned, and the target protein HAX-1 level was quantified and normalised to β-actin. The results are expressed as the mean ± SEM of three separate experiments. T vs. N. ***P<0.001, **P<0.01. (C) The results of immuno-histochemical staining (magnification, x200). The positive (brown) staining indicates the presence of the HAX-1 protein in human cervical tissues. (D) The subcellular localization of HAX-1 was detected following cellular fractionation. The SiHa cells were separated into ER, Nu and Mt fractions. Calnexin, histone Hi and mtSSB were detected by immunoblotting as markers for the ER, Nu and Mt fractions, respectively. (E) Relative HAX-1 gene expression levels were observed in the cervical squamous carcinoma cell line, HeLa, SiHa and the human cervical epithelial CRL2614 cell line. The different expression levels of HAX-1 were analysed by qPCR. (F) The expression of the HAX-1 protein was measured by western blot analysis. The graph depicts the relative HAX-1 protein levels normalised to β-actin. The results are expressed as the mean ± SEM of three separate experiments. ***P<0.001, **P<0.01, *P<0.05 vs. CRL2614 cells. HAX-1, haematopoietic cell-specific protein 1-associated protein X-1; SEM, standard error of the mean; qPCR, quantitative polymerase chain reaction; T, human cervical squamous cell carcinoma tissue; N, non-cancerous tissue; ER, endoplasmic reticulum; Nu, nuclear; Mt, mitochondrial.

staining. The expression of HAX-1 protein was detected in the endoplasmic reticulum (ER), nuclear (Nu) and mitochondrial (Mt) fractions in SiHa cells, but was primarily localized to the mitochondria (Fig. 1D). These data indicated that the expression of the HAX-1 gene may be associated with the occurrence of cervical cancer.
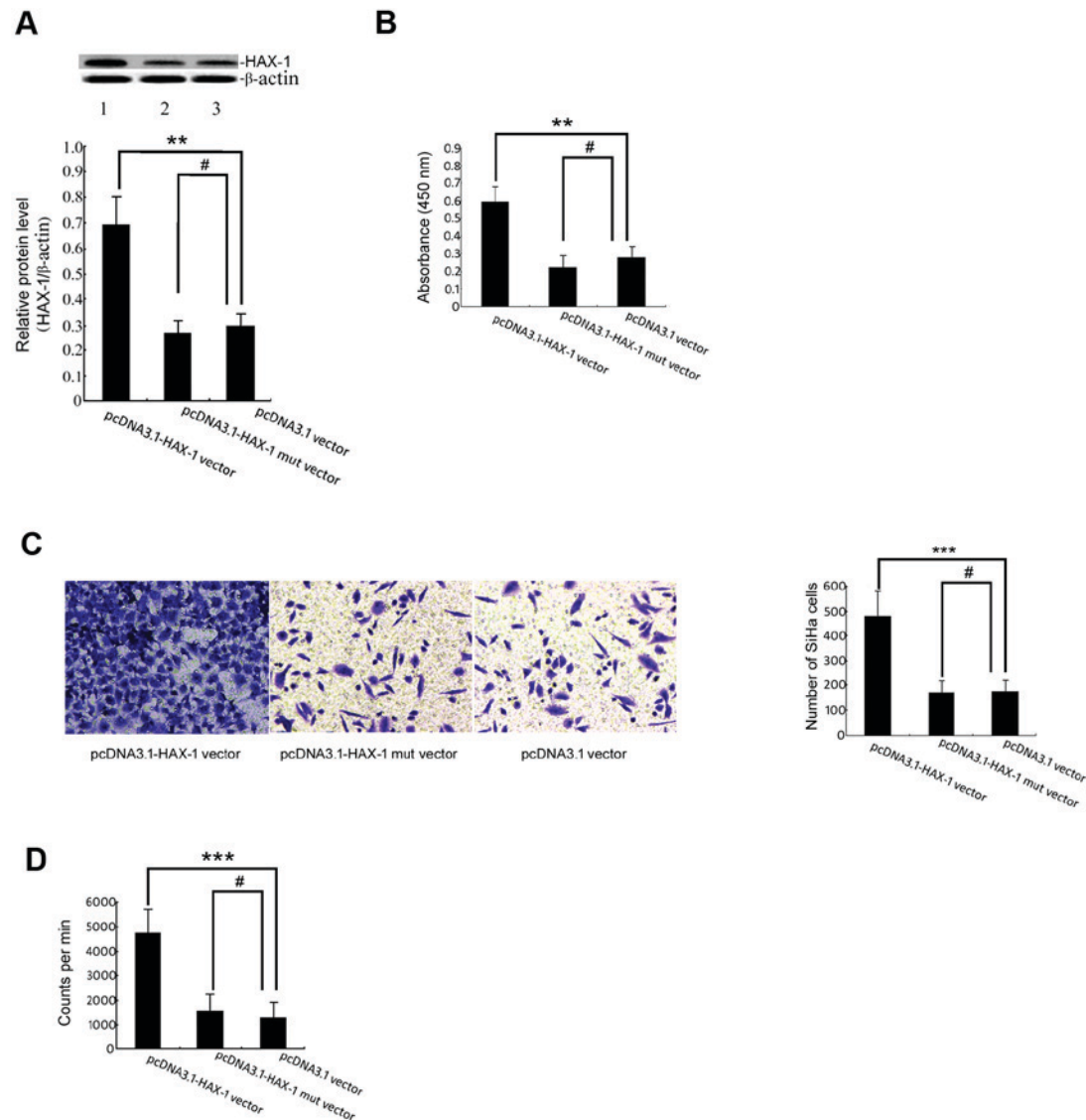
Figure 2. Effect of the HAX-1 gene on the biological function of SiHa cells. (A) The HAX-1 protein level was measured by western blot analysis. The graph was grey-scale scanned, and the target protein HAX-1 level was quantified and normalised to β-actin. The results are expressed as the mean ± SEM of three separate experiments. **P<0.01, $^{#}$P>0.05 vs. pcDNA3.1 vector groups. (B) WST-1 cell proliferation and viability. The SiHa cells were transfected with pcDNA3.1-HAX-1 vector (2 μg/ml), pcDNA3.1-HAX-1 mutated vector (2 μg/ml) and pcDNA3.1 null carrier plasmids (2 μg/ml) for 72 h before performing the WST-1 assay. The results are presented as the mean ± SEM of three independent experiments, each conducted in triplicate. **P<0.01, $^{#}$P>0.05 vs. pcDNA3.1 vector groups. (C) The effects of the HAX-1 gene on cell migration were measured by Transwell migration assay. ***P<0.001, $^{#}$P>0.05 vs. pcDNA3.1 vector groups. (D) The proliferation of SiHa cells was detected by ^{3}H-TdR incorporation. The absolute CPM value indicated the proliferation of SiHa cells (cpm/10^{6} cells). ***P<0.001, $^{#}$P>0.05 vs. pcDNA3.1 vector groups. HAX-1, haematopoietic cell-specific protein 1-associated protein X-1; SEM, standard error of the mean; WST-1, water-soluble tetrazolium salt; CPM, counts per minute.

The basal level of HAX-1 in HeLa and SiHa cells is higher than in human cervical epithelial CRL2614 cells, but the basal level of HAX-1 in SiHa cells is markedly lower than in HeLa cells (Fig. 1E and F). The SiHa cells were therefore used as the primary subject in subsequent experiments.

Effect of overexpression of HAX-1 gene on the biological behaviour of SiHa cells. The results demonstrated that the level of HAX-1 protein in the pcDNA3.1-HAX-1 vector group was significantly higher than that in the pcDNA3.1 vector group (P<0.01; Fig. 1A). The results of the WST-1 assay demonstrated that HAX-1 was able to increase the survival of SiHa cells (Fig. 2B). To determine whether HAX-1 is a regulator of SiHa cell migratory ability, Transwell experiments were performed,

which indicated that the number of HAX-1-mediated migrated SiHa cells increased markedly (Fig. 2C). The present study further utilized the ^{3}H-TdR incorporation assay to test whether HAX-1 is a regulator of SiHa cell proliferation. As demonstrated in Fig. 2D, the number of HAX-1-mediated proliferating SiHa cells increased significantly.

Effect of overexpression of the HAX-1 gene on mitochondrial function. Mitochondrial function was assessed based upon the changes in mitochondrial ROS content and Δψm. The experimental data demonstrated that the ROS production mediated by the HAX-1 gene in SiHa cells was significantly reduced (P<0.001; Fig. 3A). Additionally, the Δψm of SiHa cells induced by the HAX-1 gene did not change and maintained
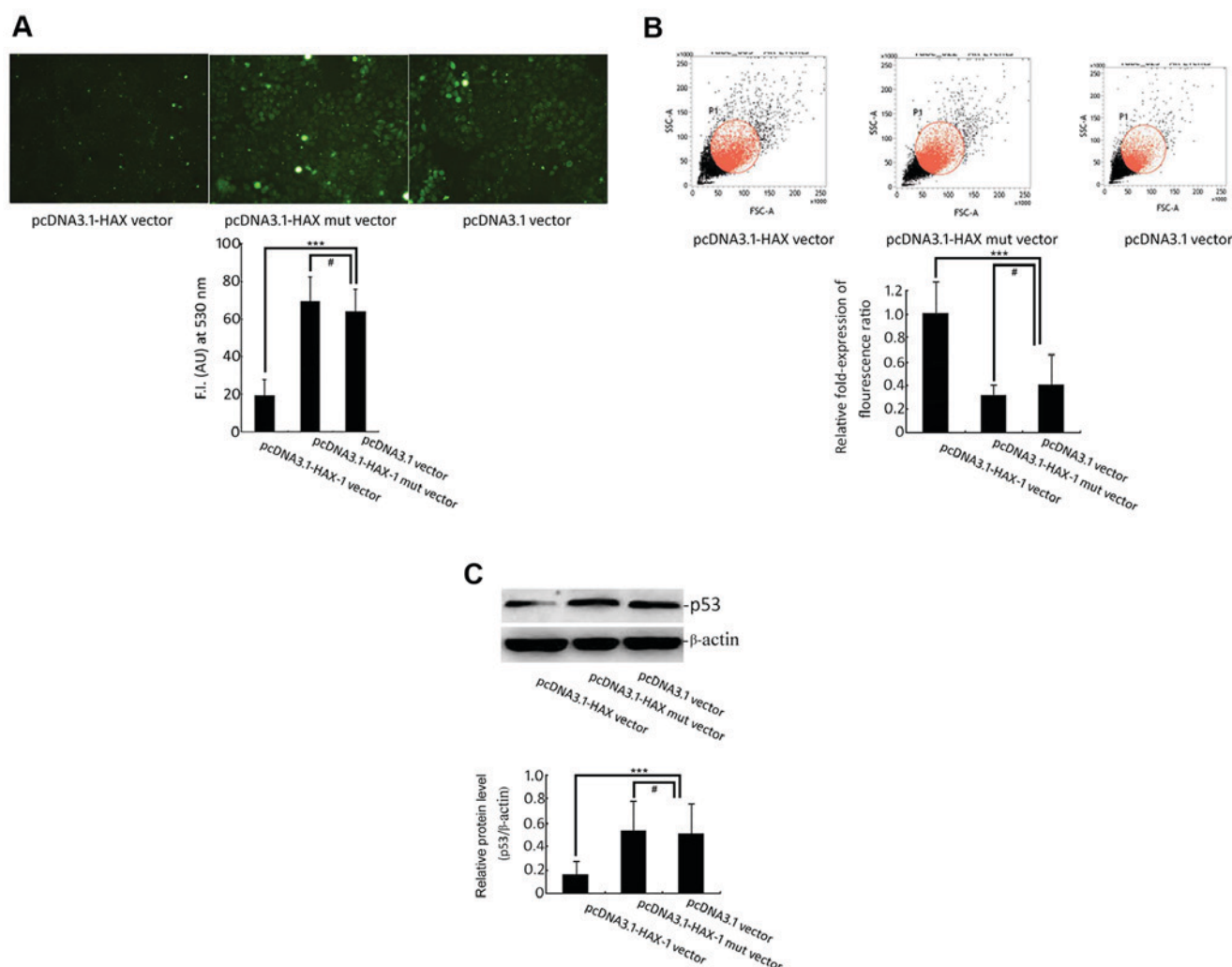
Figure 3. Effect of overexpression of the HAX-1 gene on mitochondrial function. The SiHa cells were transfected with pcDNA3.1-HAX-1 vector, pcDNA3.1-HAX-1 mutated vector or pcDNA3.1 null carrier plasmids for 48 h before the test. (A) Intracellular ROS analysis. The H_2DCFDA fluorescent probe was used to measure the changes in ROS levels by detecting changes in the fluorescence intensity of H_2DCFDA. The results are presented as the mean ± SEM. [***]P<0.001, [#]P>0.05 vs. pcDNA3.1 vector groups. (B) Mitochondrial membrane potential analysis. The Δψm value was detected by JC-1 staining. [***]P<0.001. (C) The p53 protein level was analysed by western blot analysis. The graph was grey-scale scanned, and the target protein p53 level was quantified and normalised to β-actin. The results are expressed as the mean ± SEM of three separate experiments. [***]P<0.001, [#]P>0.05 vs. pcDNA3.1 vector groups. HAX-1, haematopoietic cell-specific protein 1-associated protein X-1; ROS, reactive oxygen species; SEM, standard error of the mean; Δψm, change in mitochondrial membrane potential; p53, tumour protein P53.

complete membrane potential (Fig. 3B). However, the ROS production exhibited a significant increase, and the Δψm decreased significantly in the pcDNA 3.1-HAX-1 mutated vector group and the pcDNA3.1-null plasmid group.

The experimental western blot analysis results indicated that overexpression of the HAX-1 gene significantly inhibited the expression of p53 (Fig. 3C) and that the HAX-1 mutant did not change the expression of the p53 protein. These data indicated that the HAX-1 gene might be an upstream regulatory factor of pro-apoptotic protein p53, inhibiting the rise in its expression level.

Effect of the p53 gene on HAX-1-induced biological function in SiHa cells. These results demonstrated that HAX-1 was able to significantly increase the cell survival (Fig. 4A), migration ability (Fig. 4B) and proliferation ability (Fig. 4C) of SiHa cells, but these effects could be reversed by overexpression of the wild-type p53 gene or FCCP-induced mitochondrial

dysfunction. At the same time, these results indicated that in the pcDNA3.1-HAX-1 + wild-type p53 vector group and the pcDNA3.1-HAX-1 + FCCP group, the intracellular ROS increased significantly compared with the pcDNA3.1-HAX-1 group (P<0.01, P<0.05; Fig. 4D). However, Δψm of SiHa cells was significantly decreased in the pcDNA3.1-HAX-1 + wild-type p53 vector group and the pcDNA3.1-HAX-1 + FCCP group (P<0.01; Fig. 4E). The mitochondrial morphology indicated the presence of crista breaks that disappeared, and the stroma presented a loose state. Certain mitochondria were markedly swollen, and certain mitochondria even appeared vacuolated (Fig. 4F).

Discussion

In recent years, novel therapies for targeting receptor, gene and signal transduction in tumour formation have been emerging (16,17). Among them, the inhibition of tumour cell
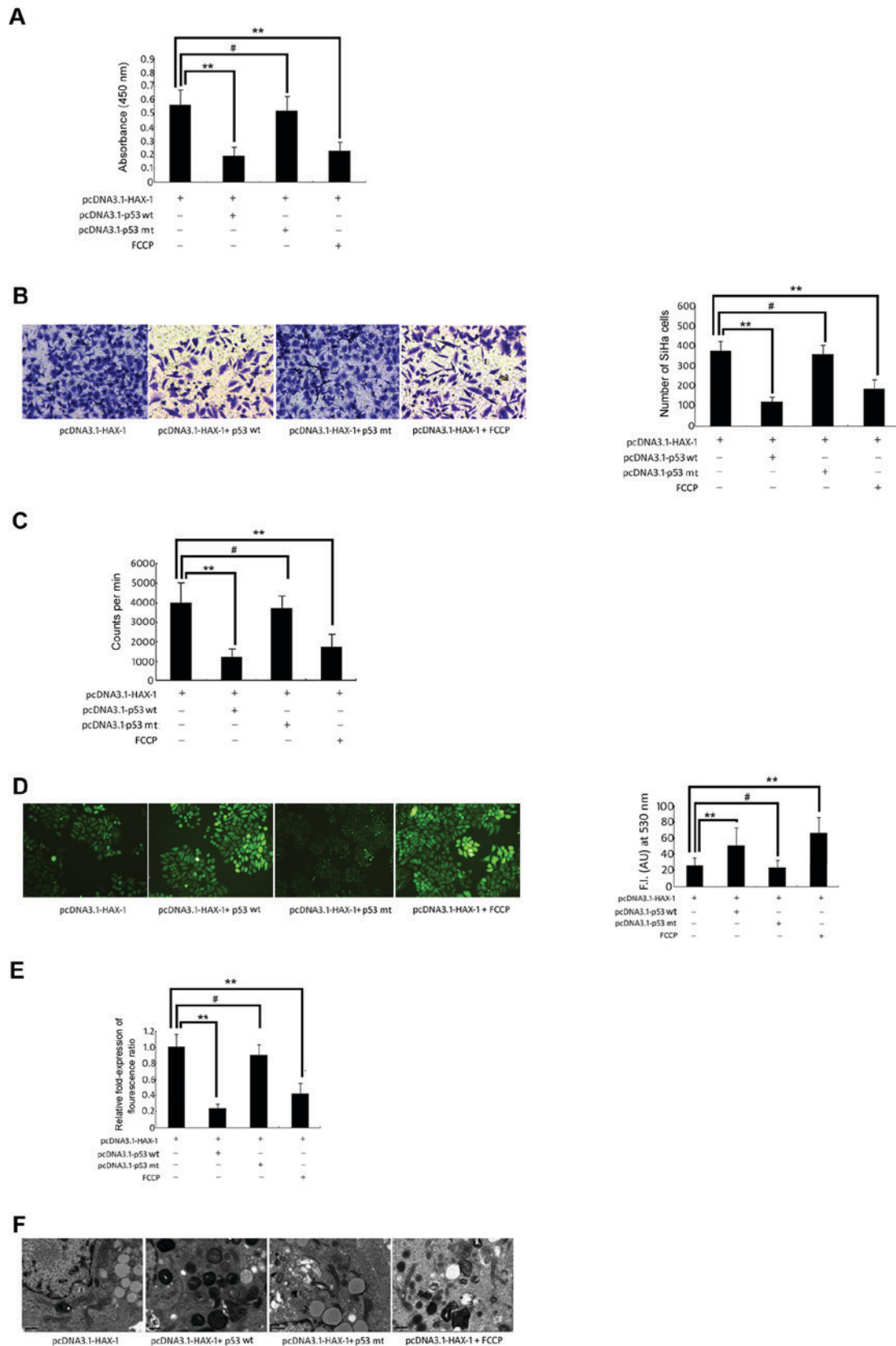
Figure 4. Change in biological function of SiHa cells. SiHa cells were co-transfected with pcDNA3.1-HAX-1 vector (2 µg/ml), pcDNA3.1-p53 wt vector (100 ng) orpcDNA3.1-p53 mut vector (100 ng), and treated with FCCP (50 µM) for 72 h. (A) The proliferative activity of SiHa cells was measured by WST-1 assay. [**]P<0.01, [#]P>0.05 vs. pcDNA3.1-HAX-1 vector groups. (B) Transwell assay was used to measure the migration of SiHa cells. [**]P<0.01, [#]P>0.05 vs. pcDNA3.1-HAX-1 vector groups. (C) The proliferation of SiHa cells was detected by ^{3}H-TdR incorporation. The cpm/10[6] cells represents the proliferative ability of SiHa cells. [**]P<0.01, [#]P>0.05 vs. pcDNA3.1-HAX-1 vector groups. (D) Reactive oxygen species generation was quantified using the H_2DCFDA fluorescence probe.[**]P<0.01, [*]P<0.05, [#]P>0.05 vs. pcDNA3.1-HAX-1 vector groups. (E) The fluorescence of JC-1 (590 nm: 527 nm fluorescence ratio) was used to calculate the relative change in mitochondrial potential value. [**]P<0.01, [#]P>0.05 vs. pcDNA3.1-HAX-1 vector groups. (F) The morphological changes of mitochondria in SiHa cells were observed by transmission electron microscopy (magnification, x12,500). HAX-1, haematopoietic cell-specific protein 1-associated protein X-1; WST-1, water-soluble tetrazolium salt; FCCP, carbonyl cyanide-p-trifluoro methoxyphenylhydrazone.

migration and proliferation is a popular research topic. A potential strategy for tumour gene therapy is to transfect apoptotic genes into tumour cells and induce their apoptosis (18), which may become a novel approach for the treatment of cervical cancer.

HAX-1 is a mitochondrial protein, which prevents the accumulation of B-cell lymphoma 2-associated X protein and apoptosis regulator (Bax), thereby inhibiting the mitochondrial apoptosis pathway (19,20). Studies have demonstrated that HAX-1 is overexpressed in cancer. The results of the present study also indicated that the HAX-1 protein is predominantly expressed in the mitochondria of cervical squamous cells (Fig. 1D). Overexpression of HAX-1 inhibits mitochondrial collapse and the subsequent release of mitochondria-derived apoptotic molecules, including cytochrome c. Apoptosis, which is usually induced by mitochondrial dysfunction, is an important target of cancer treatment (21). Mitochondrial damage results in the opening of a non-specific pore in the inner mitochondrial membrane, known as the mitochondrial permeability transition pore (mPTP). Opening of the mPTP causes the release of mitochondrial components into the cytoplasm (22). Among these components are ROS, which are key inducers of mitochondrial apoptosis (23). Therefore, the present study aimed to comprehensively determine the role of p53-induced apoptosis in the HAX-1-induced biological behaviour of cervical cancer cells and the associated mechanism of mitochondrial collapse and ROS generation.

HAX-1 acts as an anti-apoptotic protein by inhibiting the accumulation of Bax, thereby interrupting the mitochondrial apoptosis pathway (24). Previous studies have revealed that the expression of HAX-1 varies in different tumour types, including oesophageal squamous cell carcinoma (25), lung cancer, leukaemia, myeloma, breast cancer and hepatoma (26-28). Studies have reported that overexpression of HAX-1 is associated with a poor prognosis in patients with oesophageal squamous cell carcinoma (29). Therefore, HAX-1 may serve different biological roles in different tissues by modulating specific proteins and specific signalling pathways (30). In order to understand the association between the HAX-1 gene and the biological behaviour of cervical cancer cells, the cell survival rate, migration rate and proliferation rate were monitored. Following transfection of the HAX-1 expression vector into SiHa cells, the migration rate and the survival rate increased significantly. These data confirmed that HAX-1 serves an important role in promoting the survival and migration ability of cervical cancer cells. Furthermore, the HAX-1 gene may significantly reduce the accumulation of intracellular ROS, protect the mitochondrial membrane potential, and maintain the integrity of the mitochondrial structure and morphology.

As a key factor in inhibiting tumour formation, the p53 gene may be either wild-type or mutant type. The wild-type p53 gene may act as a tumour suppressor gene by repairing damaged DNA, blocking cell cycle, inhibiting cell proliferation and promoting apoptosis (31-34). However, the mutant-type p53 promotes cell proliferation through negative regulation of the wild-type p53 protein, thereby protecting cells from apoptosis and promoting tumour development. Therefore, mutant-type p53 exerts a cancer gene function (35). Over 50% of cancer cell lines evade apoptosis by mutant p53 and the other cancer cell lines also inhibit the activity of wild-type p53 by other mechanisms (36). The results of the present study demonstrated that the HAX-1 gene might significantly inhibit the p53 protein. The HAX-1 gene may be regarded as a potential upstream regulator of p53. The p53 signalling pathway has been involved in HAX-1-induced cervical cancer cell migration and proliferation. In the present study, the HAX-1 gene and wild-type p53 gene were co-transfected into cervical cancer cells. It was revealed that wild-type p53 is able to reverse the HAX-1-mediated inhibition of the production of ROS and mitochondrial membrane potential. At the same time, the wild-type p53 gene also abolished the HAX-1-induced survival and migration ability of cervical cancer cells. The aforementioned effects of wild-type p53 interfere with the HAX-1-induced biological changes, in a similar way to the effects of FCCP-induced mitochondrial dysfunction. Therefore, HAX-1 may induce the biological behaviour of cervical cancer cells through inhibiting the p53-dependent pathway.

Taken together, the results of the present study provide primary evidence that HAX-1 induced the survival, migration and proliferation of human cervical squamous carcinoma cells by inhibiting its downstream regulatory factor p53 in SiHa cells. HAX-1 therefore holds promise as a prognostic biomarker and potential therapeutic target for the treatment of cervical cancer.

Availability of data and materials

The datasets produced during and/or analysed during the current study are available from the corresponding author on reasonable request.

Authors' contributions

LJG and RS conceived and designed the experiments. BQ performed the experiments. FT, LJZ and BQ analyzed the data and contributed to the interpretation of results obtained and manuscript construction. LJG and RS edited the final draft manuscript. All authors read and approved the final manuscript.

Ethics statement and consent to participate

The present study was approved by the Ethics Committee of the Chinese Academy of Sciences and the Nanjing Maternity and Child Health Care Hospital (Nanjing, China), and written informed consent was obtained from all participants.

Consent for publication

The patient and healthy subjects provided written informed consent for the publication of any associated data and accompanying images.

Competing interests

The authors declare that they have no competing interests.

References

1. Karageorgopoulou S, Kostakis ID, Gazouli M, Markaki S, Papadimitriou M, Bournakis E, Dimopoulos MA and Papadimitriou CA: Prognostic and predictive factors in patients with metastatic or recurrent cervical cancer treated with platinum-based chemotherapy. BMC Cancer 17: 451, 2017.
2. Sodhani P, Gupta S, Gupta R and Mehrotra R: Bacterial vaginosis and cervical intraepithelial neoplasia: Is there an association or is co-existence incidental? Asian Pac J Cancer Prev 18: 1289-1292, 2017.
3. Kwon MJ, Kang SY, Nam ES, Cho SJ and Rho YS: HIPK2 overexpression and its prognostic role in human papillomavirus-positive tonsillar squamous cell carcinoma. Biomed Res Int 2017: 1056427, 2017.
4. Borcoman E and Tourneau CL: Pembrolizumab in cervical cancer: latest evidence and clinical usefulness. Ther Adv Med Oncol 9: 431-439, 2017.
5. Karan D, Tawfik O and Dubey S: Expression analysis of inflammasome sensors and implication of NLRP12 inflammasome in prostate cancer. Sci Rep 7: 4378, 2017.
6. Rosania R, Varbanova M, Wex T, Langner C, Bornschein J, Giorgio F, Ierardi E and Malfertheiner P: Regulation of apoptosis is impaired in atrophic gastritis associated with gastric cancer. BMC Gastroenterol 17: 84, 2017.
7. Shen S, Li W, Ouyang MA and Wang J: Structure-activity relationship of triterpenes and derived glycosides against cancer cells and mechanism of apoptosis induction. Nat Prod Res 32: 654-661, 2018.
8. Paech F, Bouitbir J and Krähenbühl S: Hepatocellular toxicity associated with tyrosine kinase inhibitors: Mitochondrial damage and inhibition of glycolysis. Front Pharmacol 8: 367, 2017.
9. Chen J, Wang YX, Dong MQ, Zhang B, Luo Y, Niu W and Li ZC: Reoxygenation reverses hypoxic pulmonary arterial remodeling by inducing smooth muscle cell apoptosis via reactive oxygen species-mediated mitochondrial dysfunction. J Am Heart Assoc 6: pii: e005602, 2017.
10. Frumovitz M, Burzawa JK, Byers LA, Lyons YA, Ramalingam P, Coleman RC and Brown J: Sequencing of mutational hotspots in cancer-related genes in small cell neuroendocrine cervical cancer. Gynecol Oncol 141: 588-591, 2016.
11. Yuan JY, Liu LY, Wang P, Li ZF, Ni L, Wang A, Xiao SX, Song TS and Huang C: Small-interfering RNA-mediated silencing of the MAPK p42 gene induces dual effects in HeLa cells. Oncol Lett 1: 649-655, 2010.
12. Lee SA, Kim JW, Roh JW, Choi JY, Lee KM, Yoo KY, Song YS and Kang D: Genetic polymorphisms of GSTM1, p21, p53 and HPV infection with cervical cancer in Korean women. Gynecol Oncol 93: 14-18, 2004.
13. You B, Cao X, Shao X, Ni H, Shi S, Shan Y, Gu Z and You Y: Clinical and biological significance of HAX-1 overexpression in nasopharyngeal carcinoma. Oncotarget 7: 12505-12524, 2016.
14. Wang Y, Huo X, Cao Z, Xu H, Zhu J, Qian L, Fu H and Xu B: HAX-1 is overexpressed in hepatocellular carcinoma and promotes cell proliferation. Int J Clin Exp Pathol 8: 8099-8106, 2015.
15. Livak KJ and Schmittgen TD: Analysis of relative gene expression data using real-time quantitative PCR and the 2(-Delta Delta C(T)) Method. Methods 25: 402-408, 2001.
16. Li Q, Shen F and Wang C: TUC338 promotes cell migration and invasion by targeting TIMP1 in cervical cancer. Oncol Lett 13: 4526-4532, 2017.
17. Chen AH, Qin YE, Tang WF, Tao J, Song HM and Zuo M: MiR-34a and miR-206 act as novel prognostic and therapy biomarkers in cervical cancer. Cancer Cell Int 17: 63, 2017.
18. Nishi K, Luo H, Ishikura S, Doi K, Iwaihara Y, Wills L, Baillie GS, Sakata T, Shirasawa S and Tsunoda T: Apremilast induces apoptosis of human colorectal cancer cells with mutant KRAS. Anticancer Res 37: 3833-3839, 2017.
19. Suzuki Y, Demoliere C, Kitamura D, Takeshita H, Deuschle U and Watanabe T: HAX-1, a novel intracellular protein, localized on mitochondria, directly associates with HS1, a substrate of Src family tyrosine kinases. J Immunol 158: 2736-2744, 1997.
20. Chao JR, Parganas E, Boyd K, Hong CY, Opferman JT and Ihle JN: Hax1-mediated processing of HtrA2 by Parl allows survival of lymphocytes and neurons. Nature 452: 98-102, 2008.
21. Fulda S and Debatin KM: Extrinsic versus intrinsic apoptosis pathways in anticancer chemotherapy. Oncogene 25: 4798-4811, 2006.
22. Halestrap AP, Clarke SJ and Javadov SA: Mitochondrial permeability transition pore opening during myocardial reperfusion-a target for cardioprotection. Cardiovasc Res 61: 372-385, 2004.
23. Zorov DB, Juhaszova M and Sollott SJ: Mitochondrial reactive oxygen species (ROS) and ROS-induced ROS release. Physiol Rev 94: 909-950, 2014.
24. Wu JY, Li M, Cao LJ, Sun ML, Chen D, Ren HG, Xia Q, Tao ZT, Qin ZH, Hu QS and Wang GH: Protease Omi cleaving Hax-1 protein contributes to OGD/R-induced mitochondrial damage in neuroblastoma N2a cells and cerebral injury in MCAO mice. Acta Pharmacol Sin 36: 1043-1052, 2015.
25. Li M, Tang Y, Zang W, Xuan X, Wang N, Ma Y, Wang Y, Dong Z and Zhao G: Analysis of HAX-1 gene expression in esophageal squamous cell carcinoma. Diagn Pathol 8: 47, 2013.
26. Trebinska A, Rembiszewska A, Ciosek K, Ptaszynski K, Rowinski S, Kupryjanczyk J, Siedlecki JA and Grzybowska EA: HAX-1overexpression, splicing and cellular localization in tumors. BMC Cancer 10: 76, 2010.
27. Sun X, Li Y, Zheng M, Zuo W and Zheng W: MicroRNA-223 increases the sensitivity of triple-negative breast cancer stem cells to TRAIL-induced apoptosis by targeting HAX-1. PLoS One 11: e0162754, 2016.
28. Banerjee A, Saito K, Meyer K, Banerjee S, Ait-Goughoulte M, Ray RB and Ray R: Hepatitis C virus core protein and cellular protein HAX-1 promote 5-fluorouracil-mediated hepatocyte growth inhibition. J Virol 83: 9663-9671, 2009.
29. Sun SJ, Feng L, Zhao GQ and Dong ZM: HAX-1 promotes the chemoresistance, invasion, and tumorigenicity of esophageal squamous carcinoma cells. Dig Dis Sci 57: 1838-1846, 2012.
30. Hirasaka K, Mills EM, Haruna M, Bando A, Ikeda C, Abe T, Kohno S, Nowinski SM, Lago CU, Akagi K, et al: UCP3 is associated with Hax-1 in mitochondria in the presence of calcium ion. Biochem Biophys Res Commun 472: 108-113, 2016.
31. Xia C, Shui L, Lou G, Ye B, Zhu W, Wang J, Wu S, Xu X, Mao L, Xu W, et al: 0404 inhibits hepatocellular carcinoma through a p53/miR-34a/SIRT1 positive feedback loop. Sci Rep 7: 4396, 2017.
32. Hoffman S, Martin D, Meléndez A and Bargonetti J: C. elegans CEP-1/p53 and BEC-1 are involved in DNA repair. PLoS One 9: e88828, 2014.
33. Ai G, Dachineni R, Kumar DR, Marimuthu S, Alfonso LF and Bhat GJ: Aspirin acetylates wild type and mutant p53 in colon cancer cells: Identification of aspirin acetylated sites on recombinant p53. Tumour Biol 37: 6007-6016, 2016.
34. Delbridge AR, Pang SH, Vandenberg CJ, Grabow S, Aubrey BJ, Tai L, Herold MJ and Strasser A: RAG-induced DNA lesions activate proapoptotic BIM to suppress lymphomagenesis in p53-deficient mice. J Exp Med 213: 2039-2048, 2016.
35. Iwanicki MP, Chen HY, Iavarone C, Zervantonakis IK, Muranen T, Novak M, Ince TA, Drapkin R and Brugge JS: Mutant p53 regulates ovarian cancer transformed phenotypes through autocrine matrix deposition. JCI Insight 1: e86829, 2016.
36. Wang M, Zhang Y, Wang T, Zhang J, Zhou Z, Sun Y, Wang S, Shi Y, Luan X, Zhang Y, et al: The USP7 inhibitor P5091 induces cell death in ovarian cancers with different P53 status. Cell Physiol Biochem 43: 1755-1766, 2017.